Phase-tuned neuronal firing encodes human contextual representations for navigational goals

Andrew J Watrous[1], Jonathan Miller[1], Salman E Qasim[1], Itzhak Fried[2], Joshua Jacobs[1]

1. Department of Biomedical Engineering, Columbia University, New York, NY 10027
2. Department of Neurosurgery, David Geffen School of Medicine and Semel Institute for Neuroscience and Human Behavior, University of California, Los Angeles, Los Angeles, CA 90095, USA

Abstract

We previously demonstrated that the phase of oscillations modulates neural activity representing categorical information using human intracranial recordings and high-frequency activity from local field potentials (Watrous et al., 2015b). We extend these findings here using human single-neuron recordings during a navigation task. Cells with firing rate modulations were observed primarily in entorhinal and frontal cortices. Using a novel oscillation detection algorithm, we identify phase-locked neural firing that encodes information about a person's prospective navigational goal. These results provide evidence for contextual accounts of human MTL function at the single-neuron level and identify phase-coded neuronal firing as a component of the human neural code.

Introduction

Single-neuron firing forms a fundamental basis of the neural code during perception and memory. In addition to the well-established role for behavior-related changes in neuronal firing rates, converging evidence across species and behaviors suggests that interactions between single-neuron spike timing and network oscillations observed in the local field potential (LFP) also contribute to the neural code (Hyman et al., 2005; Huxter et al., 2003; Rutishauser et al., 2010; Belitski et al., 2008; Ng et al., 2013; Kayser et al., 2009; Siegel et al., 2009). For instance, rodent hippocampal cells show phase precession relative to theta oscillations during navigation (O'Keefe & Recce, 1993; Terada et al., 2017), in which the theta phase of neuronal firing represents information about a rat's position (Jensen & Lisman, 2000). Synthesizing these findings in Spectro-Contextual Encoding and Retrieval Theory (SCERT), we have hypothesized that frequency-specific and phase-locked neuronal firing at different phases (i.e. phase coding) also forms a basis of the human neural code (Watrous & Ekstrom 2014; Watrous et al., 2015a). We previously reported evidence for SCERT (Watrous et al., 2015b) using high-frequency activity in the LFP as a proxy for single-cell spiking (Crone et al., 1998; Manning et al., 2009; Miller et al., 2014). However, given the uncertain relationship (Ekstrom et al., 2007; Rey et al., 2014) between single neurons and high-frequency activity in the human medial temporal lobe (MTL), it is unclear whether phase coding manifests in MTL neurons. We clarify this issue here by testing new aspects of SCERT, seeking to extend our previous findings of phase coding (Watrous et al., 2015b) to the single-neuron level.

Several lines of evidence indicate that the human MTL forms active representations of spatial context (Ranganath & Ritchey, 2012) such as navigational goals (Watrous et al., 2011; Brown et al., 2016), yet how such representations are instantiated at the single-neuron level remains largely unknown. Drawing upon SCERT, we hypothesized that phase-coding in single neurons also supports spatial contextual representations for prospective goals.

We analyzed a dataset that simultaneously measured human single-neuron and oscillatory activity from MTL, frontal, and lateral temporal regions during a goal-directed navigation task (Jacobs et al., 2010; Miller et al., 2015). Following the analytic strategy from our previous work (Watrous et al., 2015b), we first tested for frequency-specific phase locking and then directly tested for phase coding, which would appear as individual neurons that spiked at different phases according to the prospective goal. We examined these patterns first in the medial temporal lobe and then extratemporal areas. Our results confirmed the existence of rate and phase coding for navigational goals in individual neurons, thus providing the first evidence for the oscillatory phase coding of spatial contextual information in the human MTL.

Results

Slow theta oscillations (3Hz) in the MTL during virtual navigation

Our primary aim was to test if human MTL neurons encode behavioral information by modulating their spiking based on the phase of slow oscillations. Examining this hypothesis required that we accurately identify the presence and phase of slow oscillations, particularly because human MTL oscillations are lower frequency and less stationary compared to the stable theta oscillations observed in rodents (Watrous et al., 2013; Vass et al., 2016). We developed a novel method, the Multiple Oscillations Detection Algorithm ("MODAL"; Figure 1A-C), to detect and characterize neural oscillations in adaptively identified band(s) whose frequency ranges are customized for each recording site according to its spectral properties. MODAL identifies narrow-band oscillations exceeding the background 1/f spectrum (Figure 1A) and calculates the instantaneous phase and frequency of oscillations in each band (see Methods) while excluding timepoints without oscillations or that exhibited epileptogenic activity (Gelinas et al., 2016). Thus, MODAL allowed us to test for phase coding of spikes during the presence of narrowband oscillations.

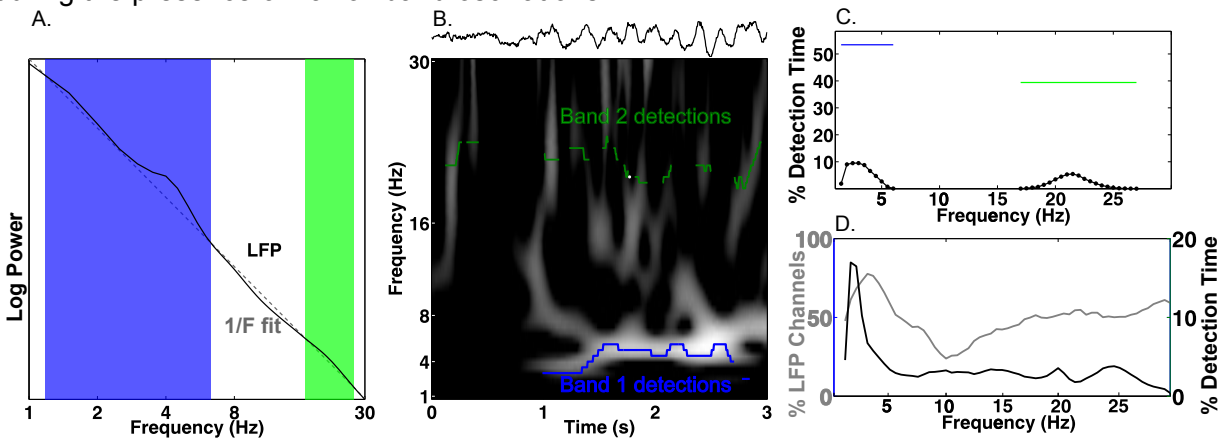

Figure 1 Multiple Oscillation Detection Algorithm ("MODAL")
A-C) Key steps in the algorithm, shown for an example electrode from the right hippocampus of patient 9. A) Mean log power averaged over time (black) and a fit line of the 1/f background spectrum (gray). A slow theta band (blue) and a beta band (green) are identified as contiguous frequencies exceeding the fit line. B) Example output from MODAL depicting a raw trace example of the LFP (upper) with the detected oscillations in each band (lower). The instantaneous frequency of the detected oscillation in each band is overlaid on a spectrogram and gray portions of the spectrogram indicate power values exceeding a local fit (similar to A but using a 10s epoch). C) Accumulating detections over time reveals the prevalence of oscillations at each frequency on this electrode (black). Blue and green bars indicate the overall prevalence of oscillations in each frequency, independent of the exact frequency within a band. D) Population data demonstrating low frequency oscillations. Grey line indicates the percent of LFP

channels with a detected band as a function of frequency. Of those channels with a detected band, the black line indicates the average amount of time each frequency was detected. Slow theta oscillations (below 5Hz) are observed using both metrics.

MODAL reliably identified oscillations at multiple frequencies that were visible in the raw trace (Figure 1B-C). Analyzing each of 385 LFP signals across the entire task period using MODAL, we found that most signals showed a band of activity centered at "slow theta" (~3Hz; 93% of signals; Figure 1D, gray line). Analyzing the overall amount of time each frequency was detected on these electrodes, we found that slow theta was detected most often (Figure 1D, black line). These results are consistent with previous work showing the prevalence of slow theta in the human MTL (Watrous et al., 2011; Watrous et al., 2013; Vass et al., 2016, Jacobs, 2014; Bohbot et al., 2017). We subsequently restricted our analysis to the low-frequency band (1–10 Hz) in order to mirror the approach from our previous work (Watrous et al., 2015b).

Phase-locked neuronal firing

We leveraged MODAL's ability to precisely track the instantaneous phase during oscillations to probe how phase coordinates the activity of individual neurons. Focusing first on the MTL, we analyzed 441 (83%) neurons that each had a simultaneously recorded LFP with an oscillation at 1–10 Hz. In many cells we observed significant phase-locking, an overall tendency for firing to increase at particular phases of the LFP oscillation (Jacobs et al., 2007; Rey et al., 2014). Phase locking is evident by examining the LFP phase distribution for all spikes which occurred during oscillations from a given cell (Figure 2A upper, Rayleigh p<.005). Across our population of recordings, we identified phase-locked neural firing in 119 neurons (111/441, 25%, Rayleigh test, p<.005), a proportion significantly above chance (Binomial p<.00001). We observed that phase locked neural firing was clustered just after the trough of the oscillation for these cells (Figure 2B, Rayleigh test p<.00001) and most phase locking occurred to slow-theta oscillations below 5 Hz (Figure 2C).

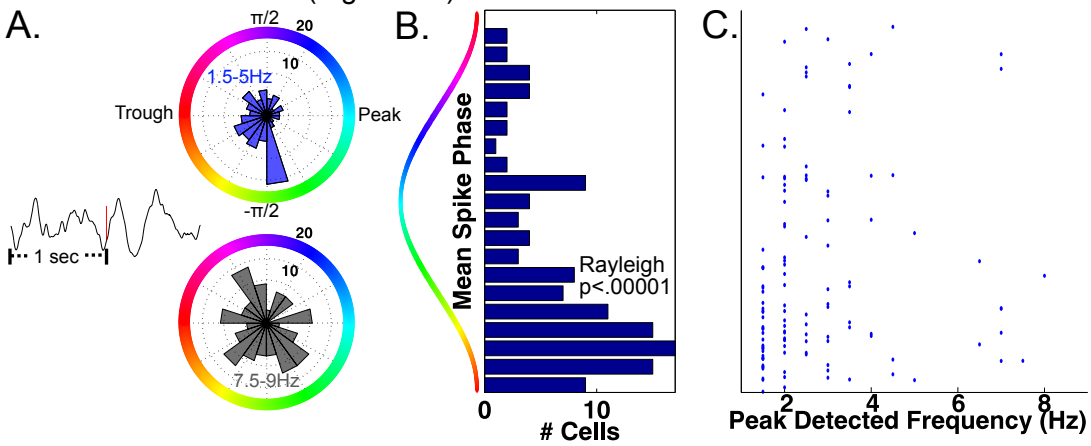

Figure 2 Phase-Locked Neural Firing
A) Spike-triggered average of a phase-locked neuron from the right hippocampus of Patient 1 (left). Red tick mark denotes a spike. Circular histograms (right) show phases at which spikes occurred relative to two detected bands. Spiking was phase-locked to the ascending phase in the 1.5-5 Hz band (red) but not in the 7.5-9 Hz band (Rayleigh test, p=.004 and p=.34, respectively). B) Population data: Pooling over frequencies, mean spike phases were significantly clustered near the initial ascending phase of the oscillation. C) Population scatter plot of the mean phase of firing and maximally detected frequency within the band for each of 119 phase-locked neurons.

The LFPs associated with 48 neurons displayed oscillations at two distinct frequency bands in the 1–10Hz range. We next tested if the spike–LFP phase locking was specific to an individual frequency band or present for both bands. 12.5% of these cells (6/48) showed frequency-specific phase locking, showing phase-locked firing in only one LFP frequency band (Figure 2a; p<.005 in one band, p>.1 in all other bands). Extending previous findings (Jacobs et al., 2007) by examining phase-locking to adaptively-identified narrowband signals, we find that human neuronal firing is modulated by the phase of low-frequency oscillations in a band and frequency-specific manner, as predicted by SCERT (Watrous & Ekstrom, 2014).

LFP-spike phase coding of goal information

Previous work has identified single neurons responsive to navigational goals (Ekstrom et al., 2003). To understand the behavioral relevance of phase-tuned neuronal activity, we tested whether neurons also used phase-tuned neural firing to encode contextual information about the patient's prospective navigational goal, analogous to the phase coding for location in the rodent hippocampus (O'Keefe & Recce, 1993). We identified 160 goal cells (36%) whose firing rates were significantly modulated by the patient's navigational goal (Figure 3A-B, all $\chi 2(5)$>, p<.0001). These cells were present in 11 of 12 patients. This result replicates previous studies implicating the MTL in the representation of navigational goals (Ekstrom et al., 2003; Watrous et al., 2011).

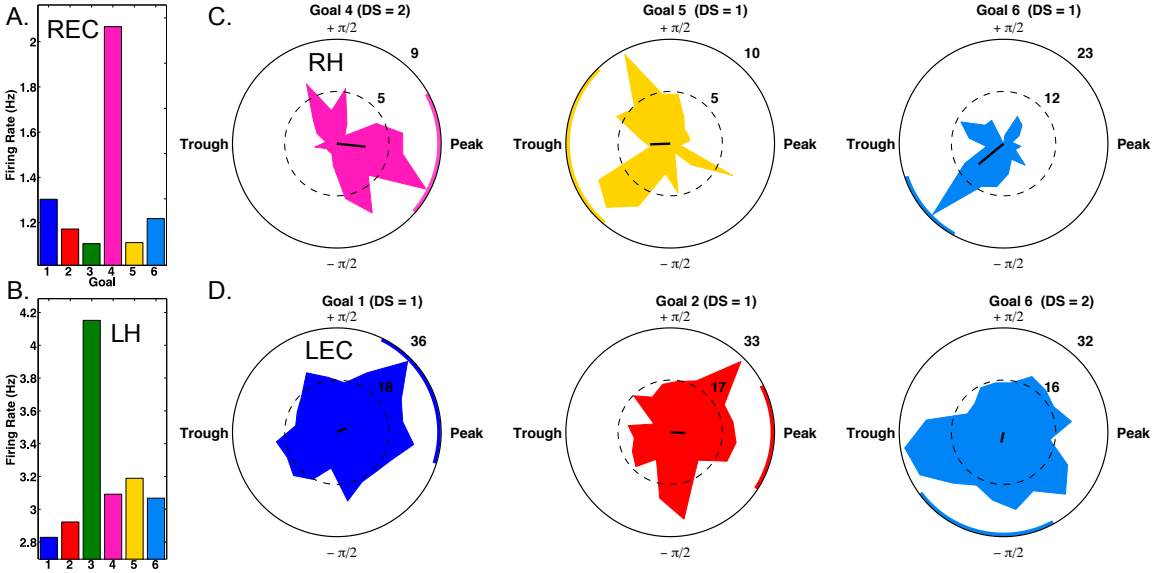

Figure 3 Example cells showing goal coding by firing rate and spike-LFP phase
A) Example neuron from patient 4 whose firing rate was significantly modulated by navigational goal (chi-square test, p<.00001) but not by spike-LFP phase (decoding p>.05, not shown). Firing rate is plotted as a function of each navigational goal. B) Another example neuron showing firing rate modulation by goal from patient 11. C) Example neuron from patient 1 showing significant spike-LFP phase coding for goal 4 (difference score (DS) = 2) compared to goals 5 and 6. Circular histograms show spike counts separately for different goals, and only goals with a difference score greater than zero are plotted for clarity. Black line at center of each plot shows the resultant vector and the colored arc indicates the 95th percentile confidence interval of the circular mean. D) Example cell from patient 6 showing phase coding for goal 6. Each cell in Figure 3 is unique and from a different patient. LEC/REC: Left/Right entorhinal cortex; LH/RH: Left/Right hippocampus

We then asked if neurons additionally represent information about the prospective goal via phase coding. We first examined the LFP phase distribution for

each cell's spiking using a difference score (DS) approach, in which we use circular statistics to compare distributions of spike phases between individual goals (Watrous et al., 2015b). This analysis revealed cells that fired at significantly different LFP phases ($p<.0001$) according to the patient's goal (Figure 3C-D). For instance, Figure 3C shows the spike–phase distribution from a right hippocampal neuron that fired preferentially near the oscillatory peak when the patient was seeking goal #4 and near the trough for goals 5 and 6. To more systematically quantify phase coding and probe whether this phenomenon is distinct from rate coding, we examined the 158 neurons whose firing rates were not goal-modulated ($p>.05$). Of these, we identified 28 neurons (17%) with significantly different spike phases for different goals (DS>0 for at least one goal), a proportion significantly above chance (Binomial test, $p<.000001$, chance = .237 cells). Thus, independent information about the patient's prospective goal could be recovered by considering the LFP phase at which these neurons fired.

To verify this interpretation and further ensure that these phase differences were robust, we used a decoding approach (Watrous et al., 2015) to test whether the patient's prospective goal could be predicted from the phase of neuronal spiking for cells that did not demonstrate rate coding. We observed significant decoding of goal information from spike phase in 19 of 158 (12%) neurons for at least one band (Binomial test, $p<.00014$, chance = 7.9 cells). Cells that exhibited phase coding of goal information were present in 7 of 12 patients. We observed a similar proportion of phase-coding neurons (67/441, 15%) when considering all neurons in our dataset, indicating that our exclusion of rate-modulated cells did not bias our results.

Finally, we explored the anatomical distribution of rate and phase-coding cells across our dataset (see Methods). We found that rate-coding cells were differentially clustered in particular regions ($\chi^2(5)=70.5$, $p<10^{-12}$). The entorhinal cortex (58% of 162 cells) and frontal cortex (44% of 355 cells) had the largest proportions of cells with firing rate modulations for goals. In contrast, phase coding cells were not significantly clustered by brain region ($\chi^2(5)=7.3$, $p=.19$). Together, these results extend our previous findings (Watrous et al., 2015b) to single neurons, providing the first evidence for single-neuron phase coding during navigation in humans.

General Discussion

Analyzing recordings from epilepsy patients performing a goal-directed navigation task, we expand our previous observation of phase-coding with high-frequency LFPs (Watrous et al., 2015b) to the domain of single neuron spiking. While we replicated the earlier finding of firing-rate coding of goal representations in human single-cell activity (Ekstrom et al., 2003), we also found a distinct population of cells in which spike-LFP phase coding contributed to representations in the absence of significant changes in firing rate (Rutishauser et al., 2010). Furthermore, we found neurons that were phase-locked to frequency-specific narrowband oscillations primarily in the slow-theta band. Together, these findings provide new, stronger evidence for the SCERT model at the single-neuron level.

Our analyses benefited from employing the MODAL algorithm, which combines features of earlier algorithms (Whitten et al., 2011; Lega et al., 2012; Cohen 2014) to identify oscillatory bands in a manner that is customized for each recording site. We believe MODAL is an improvement on these methods because it adaptively identifies oscillatory band(s) without introducing experimenter bias regarding bands of interest, excludes periods when phase is noisy because oscillations are absent, and provides exactly one estimate of phase and frequency per band.

Our findings provide the first evidence of phase coding during human navigation and provide a theoretically important link to other model systems where phase coding is

present (Siegel et al., 2009; Kayser et al., 2009; Ng et al., 2013), such as phase-precession (O'Keefe and Recce, 1993; Terada et al., 2017). However, we found prominent phase-locking and phase-coding to slower frequency oscillations below 5 Hz, suggesting that phase coding exists beyond the canonical 8-Hz theta signal seen in rats. These findings thus lend further credence to findings indicating that (virtual) navigation-related theta occurs at a slower frequency in humans (Watrous et al., 2013; Jacobs, 2014; Bohbot et al., 2017) and demonstrates that these oscillations modulate neuronal spiking.

These results align with work implicating the human MTL in spatial contextual representation (Ranganath & Ritchey, 2012) of navigational goals (Ekstrom et al., 2003; Watrous et al., 2011; Brown et al., 2016) in support of ongoing behavior (Warren et al., 2011; Yee et al., 2014) and provide further evidence that the timing of MTL activity is critical for behavior (Reber et al., 2017; Rey et al., 2014). Combined with previous human studies (Kraskov et al., 2007; Lopour et al., 2013; Watrous et al., 2015b; ten Oever & Sack, 2015), our work indicates that both firing rate and the precise timing of activity relative to LFP phase are general coding mechanisms in the human MTL across behaviors and tasks, suggesting that other types of contextual information may also be encoded using LFP phase. Future studies can build off these findings to directly assess phase coding of other types of contextual information in humans, such as phase-precession to space or time.

Methods

Neural Recordings and behavioral task

We analyzed data from 12 patients with drug-resistant epilepsy undergoing seizure monitoring (surgeries performed by I.F.). The Medical Institutional Review Board at the University of California-Los Angeles approved this study. Patients were implanted with microwire depth electrodes (Fried et al., 1999) targeting the medial temporal lobe and medial frontal lobe sites. Groups were formed for recordings in hippocampus, entorhinal cortex, parahippocampal gyrus, amygdala, frontal cortex (orbitofrontal, cingulate, motor), and lateral temporal cortices (n=214,162,65,212,355,95 neurons, respectively). Our primary analyses of 441 neurons focused on signals from hippocampal, entorhinal, and parahippocampal regions. Microwire signals were recorded at 28-32 kHz and captured LFPs and action potentials, which were spike-sorted using *wave_clus* (Quiroga et al., 2004). Signals were then downsampled to 2 kHz.

We examined data from a total of 31 recording sessions in which patients performed a virtual-taxi driver game in a circular environment. Patients were instructed to drive passengers to one of 6 goal stores in the virtual environment. The recordings and behavioral task have been detailed in prior publications that have characterized the spatial-tuning of neurons using firing rate alone (Jacobs et al., 2010; Miller et al., 2015). Here, our primary analyses in this study focused on how contextual information about navigational goals may be encoded based on firing rates and spike-LFP interactions.

Detection and Rejection of Epileptogenic signals

We implemented an automated algorithm to detect and exclude epochs of signal likely resulting from epileptic activity following prior work (Gelinas et al., 2016). We first low-pass filtered (4th order Butterworth) the signal below 80 Hz to remove any spike-contamination at high frequencies. Epochs were marked for rejection if the envelope of the unfiltered signal was 4 standard deviations above the baseline or if the envelope of the 25-80Hz bandpass filtered signal (after rectification) was 4 standard deviations above the baseline. In some cases, we noted short "bad data" epochs lasting less than

one second were not detected. We conservatively elected to exclude these epochs by marking any "good data" epoch lasting less than one second as "bad". Bad data epochs were excluded from all analyses.

Multiple Oscillations Detection Algorithm ("MODAL")

Numerous factors contribute to the presence and characteristics of band-limited neural oscillations, broadly including neuroanatomy, behavioral state, and recording equipment (Buzsaki et al., 2012). We developed an algorithm to adaptively detect and characterize neural oscillations in bands exceeding the background 1/f spectrum motivated by rodent studies that exclude periods of low amplitude theta oscillations when assessing phase coding (Lenck-Santini & Holmes, 2008). To this end, we modified the "frequency sliding" algorithm (Cohen 2014), which provides the instantaneous phase and frequency of oscillations in a band, in two important ways.

First, rather than calculating frequency sliding in *a priori* bands, we defined bands for subsequent analysis on each electrode as those frequencies exceeding the background 1/f spectrum. We calculated power values in .5Hz steps from 1 to 50 Hz using 6 cycle Morlet wavelet convolution. We then created a power spectrum by averaging values over time (and excluding bad data epochs), and fit a line to this spectrum in log-log space using *robustfit* in Matlab. Similar approaches have been used previously (Lega et al., 2012; Podvalny et al., 2015). Frequency band edges were defined as the lowest and highest frequencies in a contiguous set of frequencies which had values exceeding this fit; several bands could be detected on each electrode. We then calculated the instantaneous frequency and phase in each detected band using the "frequency sliding" algorithm (Cohen 2014).

Second, frequency sliding provides a frequency and phase estimate at every moment in time, regardless of the presence or absence of an oscillation. We ensured that phase & frequency estimates were only obtained during time periods where there was increased power in the band of interest. We recomputed the power spectrum in 10 second, non-overlapping windows and recomputed the fit line as described above. We excluded phase and frequency estimates at time points 1) in which the power was below the fit line or, 2) were during bad data epochs. Finally, we also excluded noisy frequency estimates outside of the band, which can occur based on "phase slips" (Cohen 2014). All analyses were conducted in Matlab using custom code which is available upon request.

Statistical Analyses We used Rayleigh tests to identify phase-locked neural firing, extracting the phase of the LFP during each spike in each detected frequency band. All analyses were done considering each band separately and statistical thresholding was set at $p<.005$ for each cell. This was chosen to be stricter than $p<.05$ Bonferroni-correction across the number of bands detected in the 1-10Hz range. We identified cells with firing rate modulated by navigational goal using chi-square tests. Under the null-assumption of Poisson-spiking, which is independent of navigational goal, we derived expected spike counts for each goal by multiplying total spike count by the proportion of time the goal occurred throughout the task session.

Difference scores were calculated identically to our previous work (Watrous et al., 2015b) and used the Watson-Williams test to compare phases during spikes that occurred for each goal. We again used $p<.0001$ for statistical thresholding, as it corresponded to Bonferroni-correction ($p<.05$) for the 15 pairwise combinations of 6 goals. We then used a decoding-based approach to validate our findings, employing a linear decoder with fivefold cross-validation to predict the behavioral goal from the phase of the LFP during neural spiking. We first computed the sine and cosine of the phase

values before classification following previous work (Lopour et al., 2013; Watrous et al., 2015b). Chance performance varies across cells because we classified goal information associated with the LFP phase for each spike and the distribution of spikes across goals varied between cells. We accounted for this using a permutation procedure, re-running our classification 500 times per cell using shuffled goal information (*circshift* in Matlab to maintain the temporal structure of the session) to get a surrogate distribution of classification accuracies per cell. We then obtained a p-value for classification by ranking our observed classification accuracy to the surrogate distribution; p-values less than .05 were considered significant.

To analyze the regional specificity of rate and phase coding, we expanded our analyses to our entire dataset of neurons. We used chi square tests to assess if rate coding or phase coding cells were differentially prevalent in each region.

Acknowledgements

We wish to thank the patients for their participation in this study. This work was supported by National Institutes of Health grants NS033221 and NS084017 (I.F.), MH104606 (J.J.), and National Science Foundation GRFP (S.E.Q).

References

Belitski, A., A. Gretton, C. Magri, Y. Murayama, M. A. Montemurro, N. K. Logothetis and S. Panzeri (2008). "Low-frequency local field potentials and spikes in primary visual cortex convey independent visual information." J Neurosci 28(22): 5696-5709.

Bohbot, V. M.S. Copara, J. Gotman, A.D. Ekstrom (2017). “Low-frequency theta oscillations in the human hippocampus during real-world and virtual navigation.” Nature Communications 8: 14415.

Brown, T.I., V.A. Carr,K.F. LaRocque, S.E. Favila, A.M. Gordon, B. Bowles, , J.N. Bailenson, A.D. Wagner (2016). Prospective representation of navigational goals in the human hippocampus. Science, 352:1323-1326.

Buzsaki, G., C. A. Anastassiou and C. Koch (2012). "The origin of extracellular fields and currents--EEG, ECoG, LFP and spikes." Nat Rev Neurosci 13(6): 407-420.

Buzsaki, G. and E. I. Moser (2013). "Memory, navigation and theta rhythm in the hippocampal-entorhinal system." Nat Neurosci 16(2): 130-138.

Cohen, M. X. (2014). "Fluctuations in oscillation frequency control spike timing and coordinate neural networks." J Neurosci 34(27): 8988-8998.

Crone, N.E., D.L. Miglioretti, B. Gordon, and R.P. Lesser (1998). “Functional mapping of human sensorimotor cortex with electrocorticographic spectral analysis. II. Event-related synchronization in the gamma band”. Brain, *121*(12), 2301-2315.

Ekstrom, A. D., M. J. Kahana, J. B. Caplan, T. A. Fields, E. A. Isham, E. L. Newman and I. Fried (2003). "Cellular networks underlying human spatial navigation." Nature 425(6954): 184-188.

Ekstrom, A.D., I. Viskontas, M. Kahana, J. Jacobs, K. Upchurch, S. Bookheimer, , and I. Fried (2007). “Contrasting roles of neural firing rate and local field potentials in human memory.” Hippocampus, *17*(8): 606-617.

Fried, I., C.L. Wilson, N.T. Maidment, J. Engel Jr,E. Behnke, T.A. Fields, K.A. Macdonald, J.W. Morrow, and L. Ackerson (1999). “Cerebral microdialysis combined with single-neuron and electroencephalographic recording in neurosurgical patients”. J Neurosurgery 91(4): 697-705.

Gelinas, J. N., D. Khodagholy, T. Thesen, O. Devinsky and G. Buzsaki (2016). "Interictal epileptiform discharges induce hippocampal-cortical coupling in temporal lobe epilepsy." J Neurosci 22(6): 641-648.

Huxter, J., N. Burgess and J. O'Keefe (2003). "Independent rate and temporal coding in hippocampal pyramidal cells." Nature 425(6960): 828-832.

Hyman, J. M., E. A. Zilli, A. M. Paley and M. E. Hasselmo (2005). "Medial prefrontal cortex cells show dynamic modulation with the hippocampal theta rhythm dependent on behavior." Hippocampus 15(6): 739-749.

Jacobs, J., M. J. Kahana, A. D. Ekstrom and I. Fried (2007). "Brain oscillations control timing of single-neuron activity in humans." J Neurosci 27(14): 3839-3844.

Jacobs, J., M. J. Kahana, A. D. Ekstrom, M. V. Mollison and I. Fried (2010). "A sense of direction in human entorhinal cortex." Proc Natl Acad Sci U S A 107(14): 6487-6492.

Jacobs, J. (2014). “Hippocampal theta oscillations are slower in humans than in rodents: implications for models of spatial navigation and memory.” Philos Trans R Soc Lond B Biol Sci 369(1635): 20130304.

Jensen, O. and J. E. Lisman (2000). "Position reconstruction from an ensemble of hippocampal place cells: contribution of theta phase coding." J Neurophysiol 83(5): 2602-2609.

Kayser, C., M. A. Montemurro, N. K. Logothetis and S. Panzeri (2009). "Spike-phase coding boosts and stabilizes information carried by spatial and temporal spike patterns." Neuron 61(4): 597-608.

Kraskov, A., R. Q. Quiroga, L. Reddy, I. Fried and C. Koch (2007). "Local field potentials and spikes in the human medial temporal lobe are selective to image category." J Cogn Neurosci 19(3): 479-492.

Lega, B. C., J. Jacobs and M. Kahana (2012). "Human hippocampal theta oscillations and the formation of episodic memories." Hippocampus 22(4): 748-761.

Lenck-Santini P.P., G.L. Holmes (2008). “Altered phase precession and compression of temporal sequences by place cells in epileptic rats.” J Neurosci 28(19): 5053-5062.

Lopour, B. A., A. Tavassoli, I. Fried and D. L. Ringach (2013). "Coding of information in the phase of local field potentials within human medial temporal lobe." Neuron 79(3): 594-606.

Manning J.R., J. Jacobs, I. Fried, M.J. Kahana (2009). “Broadband shifts in local field potential power spectra are correlated with single-neuron spiking in humans.” J Neuroscience 29:13613-13620.

Miller, J. F., I. Fried, N. Suthana and J. Jacobs (2015). "Repeating spatial activations in human entorhinal cortex." Curr Biol 25(8): 1080-1085.

Miller K.J., C.J. Honey, D. Hermes, R. Rao, M. denNijs, J.G. Ojemann (2014). “Broadband changes in the cortical surface potential track activation of functionally diverse neuronal populations”. Neuroimage 85:711-720.

Ng, B. S., N. K. Logothetis and C. Kayser (2013). "EEG phase patterns reflect the selectivity of neural firing." Cereb Cortex 23(2): 389-398.

O'Keefe, J. and M. L. Recce (1993). "Phase relationship between hippocampal place units and the EEG theta rhythm." Hippocampus 3(3): 317-330.

Podvalny, E., N. Noy, M. Harel, S. Bickel, G. Chechik, C. E. Schroeder, A. D. Mehta, M. Tsodyks and R. Malach (2015). "A unifying principle underlying the extracellular field potential spectral responses in the human cortex." J Neurophysiol 114(1): 505-519.

Quiroga, R. Q., Z. Nadasdy and Y. Ben-Shaul (2004). "Unsupervised spike detection and sorting with wavelets and superparamagnetic clustering." Neural Comput 16(8): 1661-1687.

Ranganath, C. and M. Ritchey (2012). "Two cortical systems for memory-guided behaviour." Nat Rev Neurosci 13(10): 713-726.

Reber, T.P., J. Faber, J. Niediek, J Boström, C.E. Elger, and F. Mormann, (2017). “Single-Neuron Correlates of Conscious Perception in the Human Medial Temporal Lobe”. Current Biology.

Rey, H. G., I. Fried and R. Quian Quiroga (2014). "Timing of single-neuron and local field potential responses in the human medial temporal lobe." Curr Biol 24(3): 299-304.

Rutishauser, U., I. B. Ross, A. N. Mamelak and E. M. Schuman (2010). "Human memory strength is predicted by theta-frequency phase-locking of single neurons." Nature 464(7290): 903-907.

Siegel, M., M.R. Warden, and E.K. Miller (2009) “Phase-dependent neuronal coding of objects in short-term memory” PNAS 106(50) 21341-21346.

ten Oever, S. and A.T. Sack (2015). “Oscillatory phase shapes syllable perception”. Proceedings of the National Academy of Sciences, 112(52), 15833-15837.

Terada, S., Y. Sakurai, H. Nakahara and S. Fujisawa (2017). "Temporal and Rate Coding for Discrete Event Sequences in the Hippocampus." Neuron 94(6): 1248-1262.e1244.

Vass, L. K., M. S. Copara, M. Seyal, K. Shahlaie, S. T. Farias, P. Y. Shen and A. D. Ekstrom (2016). "Oscillations Go the Distance: Low-Frequency Human Hippocampal

Oscillations Code Spatial Distance in the Absence of Sensory Cues during Teleportation." Neuron 89(6): 1180-1186.

Warren, D. E., M. C. Duff, U. Jensen, D. Tranel and N. J. Cohen (2012). "Hiding in plain view: lesions of the medial temporal lobe impair online representation." Hippocampus 22(7): 1577-1588.

Watrous, A. J., J. Fell, A. D. Ekstrom and N. Axmacher (2015a). "More than spikes: common oscillatory mechanisms for content specific neural representations during perception and memory." Curr Opin Neurobiol 31: 33-39.

Watrous, A. J., L. Deuker, J. Fell and N. Axmacher (2015b). "Phase-amplitude coupling supports phase coding in human ECoG." Elife 4.

Watrous, A. J. and A. D. Ekstrom (2014). "The spectro-contextual encoding and retrieval theory of episodic memory." Front Hum Neurosci 8: 75.

Watrous, A. J., I. Fried and A. D. Ekstrom (2011). "Behavioral correlates of human hippocampal delta and theta oscillations during navigation." J Neurophysiol 105(4): 1747-1755.

Watrous, A. J., D. J. Lee, A. Izadi, G. G. Gurkoff, K. Shahlaie and A. D. Ekstrom (2013). "A comparative study of human and rat hippocampal low-frequency oscillations during spatial navigation." Hippocampus 23(8): 656-661.

Whitten, T.A., A.M. Hughes, C.T. Dickson, J.R. Caplan (2011). “A better oscillation detection method robustly extracts EEG rhythms across brain state changes: the human alpha rhythm as a test case.” Neuroimage 54(2)860-874.

Yee, L. T., D. E. Warren, J. L. Voss, M. C. Duff, D. Tranel and N. J. Cohen (2014). "The hippocampus uses information just encountered to guide efficient ongoing behavior." Hippocampus 24(2): 154-164.